Original Article

Comparison between computed tomography multislice and high-field magnetic resonance in the diagnostic evaluation of patients with renal masses

Diana Baldari[1], Sergio Capece[1], Pier Paolo Mainenti[2], Anna Giacoma Tucci[1], Michele Klain[1], Immacolata Cozzolino[1], Marco Salvatore[3], Simone Maurea[1]

[1]Department of Advanced Biomedical Sciences, University of Naples Federico II, Naples, Italy; [2]Istituto di Biostrutture e Bioimmagini (IBB), Consiglio Nazionale delle Ricerche (CNR), Naples, Italy; [3]IRCCS SDN, Naples, Italy

Correspondence to: Simone Maurea. Department of Advanced Biomedical Sciences, University of Naples Federico II, Corso Umberto I, 40 bis, 80138 Naples, Italy. Email: maurea@unina.it.

Background: Renal masses are a common finding in diagnostic imaging; these lesions usually are solid or cystic, benign or malignant, and the correct diagnosis may be difficult. The aim of our study was the comparison of multi-slice computed tomography (MSCT) and high-field magnetic resonance (MR) in the diagnostic evaluation of renal masses.

Methods: We studied 29 patients, 16 men and 13 women aged 8-85 years (mean 61±17 years) with histo-cytological diagnosis of renal masses (n=31), of which the majority (74%; n=23) was represented by malignant lesions [renal cell carcinoma (Ca) =16, chromophobe renal cell Ca =2, squamous cell Ca =1, urothelial Ca =2, lymphoma =1, Wilms tumor =1]; the remaining 8 masses (26%) were benign (pyelonephritis =2, simple cyst =1, hematic cyst =1, lipoma =1 and oncocytoma =3). All patients underwent MSCT and MR (3.0 Tesla) before and after contrast injection; the images were evaluated in double-blind by two expert radiologists. The results of the images were then compared with the histo-cytological data to calculate the values of diagnostic accuracy for both methods in the identification and characterization of renal masses. The benign or malignant nature of the lesions was established according to the regularity of the margins, presence or absence of significant contrast enhancement, infiltration of perirenal fat and vascular invasion. The concordance of the results of the two imaging techniques was then calculated using the coefficient Kappa Cohen.

Results: For both identification and characterization of renal masses, MSCT and MR showed comparable values of diagnostic accuracy with a significant concordance (k=1); in particular, the diagnostic accuracy of MSCT/MR was 100%/100% for lesion identification, 90%/90% for lesion characterization in terms of benign or malignant nature, 97%/97% for the evaluation of lesion edges, 90%/90% for the assessment of lesion contrast enhancement, 93%/93% for the evaluation of peri-renal fat infiltration and 96%/96% for the evaluation of vascular infiltration. Only in three cases of oncocytoma the two imaging methods were both inaccurate for diagnosis of benignity classifying the lesions as probably malignant on the basis of the absence of central scar and of dynamic contrast enhancement pattern.

Conclusions: The results of our study show comparable diagnostic accuracy of computed tomography (CT) and MR for the identification and characterization of expansive renal lesions. High-field MR is, therefore, a valid alternative to MSCT in the evaluation of renal masses avoiding exposure to ionizing radiation.

Keywords: Multi-slice computed tomography (MSCT); magnetic resonance (MR); renal masses; identification; characterization

Submitted Mar 21, 2015. Accepted for publication Jun 05, 2015.
doi: 10.3978/j.issn.2223-4292.2015.07.03
View this article at: http://dx.doi.org/10.3978/j.issn.2223-4292.2015.07.03

Introduction

Renal masses are diagnostic imaging evidence frequently found in clinical practice and include solid or cystic type lesions, benign or malignant; whose differential diagnosis could be complex (1). Simple cysts are the most frequent masses and these are in about 50% of the population over 50 years; these lesions may be complicated by contextual hemorrhages or infections that make them even more difficult to diagnose. Furthermore, approximately 10% of renal cell carcinomas (Ca) at first could be shown as a simple or complex cyst (2,3). The most common benign tumor mass of the kidney are oncocytoma and angiomyolipoma; oncocytoma represents about 5% of cortical renal masses and the differential diagnosis of renal cell Ca is not always easy (4). Renal cell Ca is the most common malignant solid renal mass, representing about 2-3% of all cancers of people in adulthood especially in 60-70 years old men (5); in particular, there are different kinds of renal cell Ca: the clear cell type is histologically the most frequent, while papillary Ca, chromophobe Ca and collecting duct Ca are rarer. Other tumor lesions are transitional cell Ca; these represent about 10% of upper urinary tract tumors and Wilms' tumor of childhood (6); although rarely observed (1%), medullary Ca of the kidney shows a particularly poor prognosis (7); finally, lymphomas and metastasis could involve a hard differential diagnosis. Diagnostic imaging techniques play a key role in the identification of renal masses in terms of tumor detection, lesion staging and post-treatment follow-up evaluation. Diagnostic imaging provides different modalities such as ultrasound, computed tomography (CT) and magnetic resonance (MR). CT at present is the gold standard in the characterization and staging of renal masses (8); in particular, CT shows a high diagnostic sensitivity in the identification of small lesions due to the excellent spatial resolution of the latest generation equipment with multi-detector or multi-slices technology (MDCT). MR has been proposed as an alternative technique to CT scan as the new MR equipment with high-intensity magnetic fields offers excellent image quality; in particular, MR multi-planarity without ionizing radiation is really favorable for the study of the upper abdomen (9). For these reasons, MR is currently performed in unclear cases as problem-solving imaging study, as alternative technique to CT; limited studies have shown similar diagnostic accuracy of MR compared to CT (10-13). In this study we report our experience regarding the comparison of MDCT and MRI high-field results to assess the identification and characterization of renal masses.

Materials and methods

Population

We included in our retrospective study, 29 patients (16 males and 13 females) ranging in age from 8 to 85 years (mean 61±17 years) with histological (n=30) or cytological (n=1) diagnosis of renal masses; all patients underwent CT and MR studies within the same week. A total of 31 renal masses were evaluated since a double lesion was observed in 2 patients. The majority of the lesions was malignant (74%; n=23) and with different histological type: renal cell Ca (n=16), chromophobe renal cell Ca (n=2), squamous cell Ca (n=1), urothelial Ca (n=2), lymphoma (n=1), Wilms tumor (n=1); in the remaining 8 masses (26%) expansive benign lesions were found as follow: focal pyelonephritis (n=2), simple cyst (n=1), hematic cysts (n=1), lipoma (n=1) and oncocytoma (n=3); patient clinical characteristics are shown in *Table 1*.

Computed tomography

The examinations were performed with a Toshiba Aquilon 64 slices scanner; venous access to inject the contrast was positioned in an antecubital vein of the arm by means of an 18-20 gouge-needle cannula. The first acquisition without the injection of contrast was performed at the level of the upper abdomen in cranio-caudal direction from the diaphragm to the iliac crests using the following technical parameters: collimation =16×1, pitch =0.875, kV =120, mAs =260 and field of view (FOV) =25 cm. Three scans were performed after intravenous injection of nonionic water-soluble iodinated contrast (iopromid Ultravist Schering) again in cranio-caudal direction according to the parameters: collimation =16×1, reconstruction interval =1.25 mm, pitch =0.875, kV =120, mAs=260, FOV =25 cm; the post-contrastographic acquisitions were synchronized by the "bolus tracking" technique in corticomedullary phase (40-55 s), nephrographic phase (90-120 s) and excretory phase (about 5 min); in all patients 100-130 mL of contrast (1.5 mL/kg) with a iodine concentration of 370 mg/mL were injected with automatic injector at 2-3 mL/s speed.

Magnetic resonance

MR study was performed using a high-field (3 Tesla) scanner

Table 1 Characteristics of the patient population

Patient	Age (years)	Sex (M/F)	Location	Cyto-histological type
1	75	M	Right kidney	Clear cell renal cell carcinoma
2	62	M	Right kidney	Clear cell renal cell carcinoma
			Left kidney	Clear cell renal cell carcinoma
3	45	F	Right kidney	Lipoma
4	82	F	Right kidney	Clear cell renal cell carcinoma
5	39	F	Right kidney	Clear cell renal cell carcinoma
6	69	F	Right kidney	Clear cell renal cell carcinoma
7	66	F	Left kidney	Urothelial carcinoma
8	69	M	Right kidney	Chromophobe renal cell carcinoma
9	81	F	Left kidney	Focal pyelonephritis
10	45	M	Left kidney	Ematic cyst
			Left kidney	Simple cyst
11	85	M	Left kidney	Urothelial carcinoma
12	32	M	Left kidney	Chromophobe renal cell carcinoma
13	80	F	Right kidney	Lymphoma
14	68	M	Right kidney	Clear cell renal cell carcinoma
15	65	M	Right kidney	Clear cell renal cell carcinoma
16	64	F	Right kidney	Oncocytoma
17	59	M	Right kidney	Clear cell renal cell carcinoma
18	8	F	Left kidney	Wilms tumor
19	74	M	Left kidney	Clear cell renal cell carcinoma
20	63	M	Left kidney	Squamous cell carcinoma
21	41	M	Right kidney	Focal pyelonephritis
22	62	F	Right kidney	Oncocytoma
23	75	M	Right kidney	Clear cell papillary renal cell carcinoma
24	71	M	Right kidney	Clear cell renal cell carcinoma
25	62	F	Right kidney	Oncociyoma
26	74	M	Left kidney	Clear cell renal cell carcinoma
27	66	F	Left kidney	Clear cell renal cell carcinoma
28	51	F	Right kidney	Clear cell renal cell carcinoma
29	66	M	Right kidney	Clear cell renal cell carcinoma

M, male; F, female.

(Trio, Siemens) using a body antenna with four channels; the following sequences were acquired: T1 weighted (in phase: TR/TE =1,500/2 ms; out-phase: TR/TE =1,530/35 ms) on the axial plane; T2 weighted HASTE axial and coronal planes (TR/TE =2,000/92 ms) with and without fat saturation; T2 weighted TRUFI (TR/TE =510.3/1.2 ms) on axial and coronal planes; T1 weighted VIBE (TR/TE =3.3/1.1 ms) on the axial plane before and after intravenous injection of paramagnetic contrast (gadopentic acid, Bayer HealthCare Pharmaceuticals); in all patients 10-14 mL of the contrast (0.2 mL/kg) with automatic injector at a 1.5-3 mL/s speed were injected; images in corticomedullary phase (40-55 s) nephrographic phase (90-120 s) and excretory phase (about 5 min) were performed.

Imaging analysis

For both CT and MR methods, images were evaluated

Table 2 Size of the individual masses as measured by both CT and MR

Masses	Size CT (mm)	Size MR (mm)
1	120×170	115×160
2	47×36	46×36
3	23×24	20×17
4	190×140	191×137
5	39×23	36×20
6	20×23	20×20
7	35×30	34×25
8	28×20	28×18
9	19×18	14×16
10	51×44	50×44
11	37×30	36×30
12	22×16	24×16
13	42×31	54×51
14	150×130	140×130
15	65×56	60×30
16	15×11	14×11
17	100×90	90×90
18	26×18	24×15
19	30×30	31×33
20	120×100	115×95
21	60×60	55×55
22	100×45	100×48
23	125×95	115×90
24	28×26	28×25
25	21×17	20×17
26	31×25	32×25
27	50×50	50×50
28	70×65	70×65
29	27×20	22×20
30	90×70	90×70
31	61×52	62×52

CT, computed tomography; MR, magnetic resonance.

by two radiologists with at least 5 years of experience in imaging of the abdomen, not aware of the patient history nor clinical-instrumental and histo-cytological data. In case of discordance in image interpretation between the two radiologists, a third evaluator was consulted. For lesion identification, radiologists had to report the presence or absence of changes of the renal parenchyma in terms of space-occupying lesions and they had to measure the mass size using T2-weighted MR axial images. For lesion characterization, the appearance of renal mass was rated in terms of structure, regularity or not of margins (encapsulated or unencapsulated), lesion contrast enhancement, presence or absence of infiltration of the peri-renal fat and/or of loco-regional vascular structures; the radiologists made a semi-quantitative evaluation regarding the benign or malignant nature of the lesions using a score from 0 to 7 based on following characteristic: lesion structure (simple cyst =1; cysts with nodule =2; cysts with thin septa =3a; cysts with thick septa =3b; complicated cysts =4; solid =5; mixed =6; solid with central scar =7), regularity or not of the margins (regular =0; irregular =1), lesion contrast enhancement (no significant contrast enhancement =0, significant contrast enhancement =1), infiltration or not of the peri-renal fat and loco-regional vascular structures (absent =0, present =1). A lesion was considered benign on the basis of structural characteristics according to the following scores 1, 3a, 4 and 7, as well as on the basis of margin regularity (score 0), absence of significant contrast enhancement (score 0), fat and vascular structures infiltration (score 0). Conversely, a lesion was considered malignant on the basis of structural characteristics according to the following scores 2, 3b, 5 and 6, as well as on the basis of irregular margins (score 1) and/or of the presence of significant contrast enhancement (score 1), fat and/or vascular structures infiltration (score 1). Successively, imaging results were compared with histological data for the analysis of diagnostic accuracy values regarding the identification and characterization of renal masses as benign or malignant; the concordance of the results of the two imaging methods was calculated using Cohen's Kappa coefficient.

Results

The analysis of the results obtained by both imaging techniques allowed the correct identification of all 31 renal masses with a diagnostic accuracy of 100% and a significant concordance between the two methods (k=1). *Table 2* shows the size of the individual masses as measured by both CT and MR. For to the characterization of renal masses as benign or malignant, 5/8 (63%) benign lesions were correctly characterized by both imaging methods: 1 simple cyst, 1 hematic cyst, 1 lipoma and 2 abscess pyelonephritis; conversely, all 23 malignant renal lesions were correctly characterized by both imaging methods (*Figures 1,2*).

In three cases of oncocytoma, lesions were incorrectly characterized as malignant by both CT and MR with

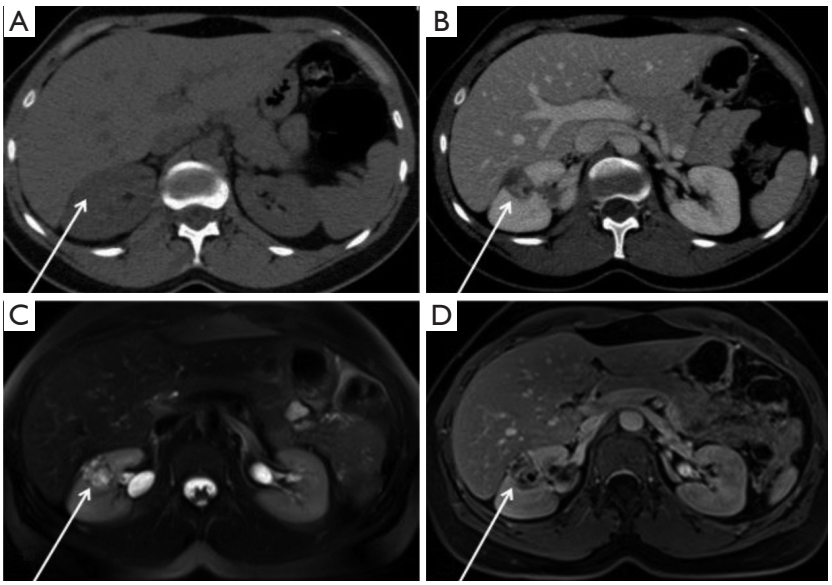

Figure 1 Patient No. 5. Transverse CT and MR scans in a patient with clear cell renal cell carcinoma. (A) Unenhanced CT image shows only the irregular profile of anterior region of the right kidney with no definite abnormality; (B) contrast-enhanced CT scan shows heterogeneus hyperenhancing by the lesion; (C) transverse fat-suppressed T2-weighted MR image shows heterogeneus signal hyperintesity by the lesion; (D) gadolinium-enhanced fat- suppressed T1-weighted MR image shows heterogeneus hyperenhancing by the lesion. CT, computed tomography; MR, magnetic resonance.

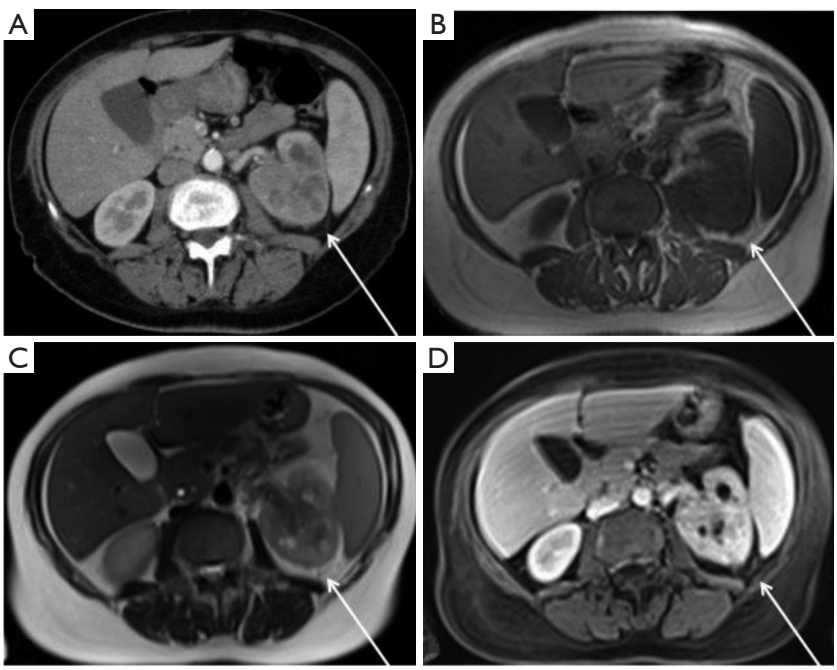

Figure 2 Patient No. 7. Transverse CT and MR scans in a patient with urothelial carcinoma. The tumor is located into the renal hilum, infiltrating into the hilum fat and the renal cortex, causing an irregolar renal profile. (A) Contrast-enhanced CT scan shows the lesion of the left kideny; (B,C) transverse T1 and T2-weighted MR images show irregular profile of left kidney and peri-renal fat infiltration; (D) gadolinium-enhanced fat- suppressed T1-weighted MR image shows malignant enhancement of peri-renal fat. CT, computed tomography; MR, magnetic resonance.

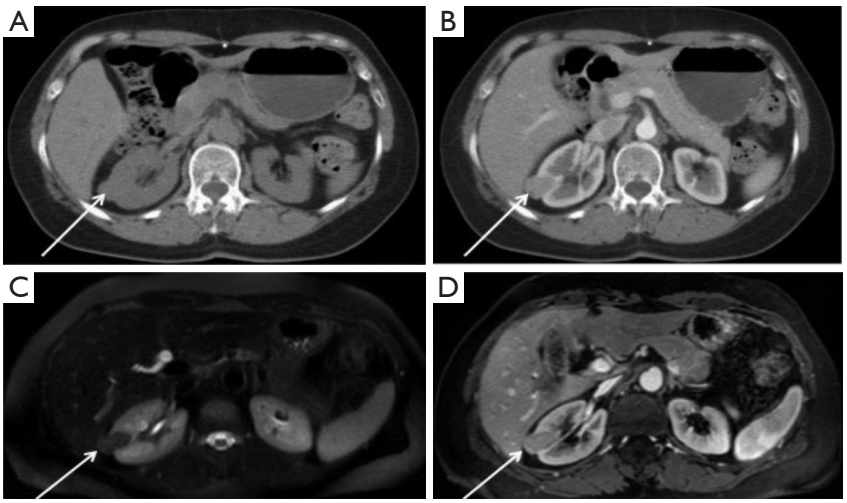

Figure 3 Patient No. 16. Transverse CT and MR scans in a patient with oncocytoma. (A) Unenhanced CT image shows an exophytic mass in the lateral interpolar region of the right kidney; (B) contrast-enhanced CT scan shows a slight enhancement by the lesion; (C) transverse fat-suppressed T2-weighted MR image shows a mass with hypointensity signal; (D) gadolinium-enhanced fat-suppressed T1-weighted MR image shows a slight enhancement by the lesion. CT, computed tomography; MR, magnetic resonance.

Table 3 Results of CT and MR for the characterization of renal masses compared with cyto-histological data

Masses	Cyto-histological type	CT	MR
1	Clear cell renal cell carcinoma	TP	TP
2	Clear cell renal cell carcinoma	TP	TP
3	Clear cell renal cell carcinoma	TP	TP
4	Lipoma	TP	TP
5	Clear cell renal cell carcinoma	TP	TP
6	Clear cell renal cell carcinoma	TP	TP
7	Clear cell renal cell carcinoma	TP	TP
8	Urothelial carcinoma	TP	TP
9	Chromophobe renal cell carcinoma	TP	TP
10	Focal pyelonephritis	TP	TP
11	Ematic cysts	TP	TP
12	Simple cyst	TP	TP
13	Urothelial carcinoma	TP	TP
14	Chromophobe renal cell carcinoma	TP	TP
15	Lymphoma	TP	TP
16	Clear cell renal cell carcinoma	TP	TP
17	Clear cell renal cell carcinoma	TP	TP
18	Oncocytoma	FP	FP
19	Clear cell renal cell carcinoma	TP	TP
20	Wilms tumor	TP	TP
21	Clear cell renal cell carcinoma	TP	TP
22	Squamous cell carcinoma	TP	TP
23	Focal pyelonephritis	TP	TP
24	Oncocytoma	FP	FP
25	Clear cell papillary renal cell carcinoma	TP	TP
26	Clear cell renal cell carcinoma	TP	TP
27	Oncocytoma	FP	FP
28	Clear cell renal cell carcinoma	TP	TP
29	Clear cell renal cell carcinoma	TP	TP
30	Clear cell renal cell carcinoma	TP	TP
31	Clear cell renal cell carcinoma	TP	TP

TP, true positive; FP, false positive; CT, computed tomography; MR, magnetic resonance.

a diagnostic accuracy of 90% (*Figure 3*). *Tables 3-5* show the results of the two imaging techniques for the characterization for each lesion. CT and MR showed comparable diagnostic accuracy values with a significant concordance (k=1) both for the evaluation of lesion margins and contrast enhancement, as well as perirenal fat and loco-regional vascular structures infiltration.

Discussion

The results of our study have shown similar diagnostic

Table 4 Results of CT and MR for the evaluation of lesion margins, lesion contrast enhancement, perirenal fat and loco-regional vascular structures infiltration and lesion structure

Masses	Margins*		Contrast enhancement**		Peri-renal fat infiltration***		Loco-regional vascular structures infiltration***		Lesion structure****	
	CT	MR	CT	MR	CT	MR	CT	MR	CT	MR
1	1	1	1	1	0	0	0	0	2	2
2	0	0	1	1	0	0	0	0	5	5
3	0	0	1	1	0	0	0	0	5	5
4	0	0	0	0	0	0	0	0	5	5
5	0	0	1	1	0	0	0	0	5	5
6	0	0	1	1	0	0	0	0	3	3
7	0	0	1	1	0	0	0	0	5	5
8	1	1	1	1	1	1	0	0	5	5
9	0	0	1	1	0	0	0	0	5	5
10	1	1	0	0	1	1	0	0	6	6
11	0	0	0	0	0	0	0	0	4	4
12	0	0	0	0	0	0	0	0	1	1
13	1	1	1	1	1	1	1	1	5	5
14	0	0	1	1	0	0	0	0	6	6
15	1	1	1	1	1	1	1	1	5	5
16	0	0	1	1	0	0	0	0	5	5
17	1	1	1	1	1	1	0	0	5	5
18	0	0	1	1	0	0	0	0	5	5
19	0	0	1	1	0	0	0	0	5	5
20	0	0	1	1	0	0	0	0	5	5
21	0	0	1	1	0	0	0	0	5	5
22	1	1	1	1	1	1	0	0	6	6
23	0	0	0	0	0	0	0	0	1	1
24	0	0	1	1	0	0	0	0	5	5
25	0	0	1	1	0	0	0	0	5	5
26	0	0	1	1	1	1	0	0	5	5
27	0	0	1	1	0	0	0	0	6	6
28	0	0	1	1	0	0	0	0	6	6
29	0	0	1	1	0	0	0	0	5	5
30	1	1	1	1	1	1	0	0	6	6
31	1	1	1	1	0	0	0	0	6	6

*: 0, regular; 1, irregular. **: 0, non-significant; 1, significant. ***: 0, absent; 1, present. ****: 1, simple cyst; 2, cysts with nodule; 4, complicated cysts; 5, solid; 6, mixed; CT, computed tomography; MR, magnetic resonance.

accuracy of CT and MR both for lesion identification and characterization in patients with renal masses. Currently, despite the availability of various imaging techniques such as ultrasound, CT and MR, the majority of renal masses are identified at an advanced stage. It happens because these kinds of lesions generally do not show significant signs and symptoms for a long time. Ultrasonography is routinely used as the first level diagnostic imaging modality because it is widespread, non-invasive and has no side effects; furthermore, in optimal conditions ultrasound

Table 5 Diagnostic accuracy values and concordance between the two methods

Variables	CT	MR	k
Lesion identification	100	100	1
Lesion characterization	90	90	1
Margins	97	97	1
Contrast enhancement	90	90	1
Peri-renal fat infiltration	93	93	1
Loco-regional vascular structures infiltration	96	96	1

CT, computed tomography; MR, magnetic resonance.

allows a good loco-regional evaluation of the upper abdomen providing anatomic details regarding kidney morphology, renal parenchymal structure and vascular analysis using color-Doppler; however, technical limitations of ultrasound are well known such as operator-experience, patient obesity and/or intestinal bloating. Therefore, it is usually necessary a second level diagnostic test such as CT and/or MR; in this regard, CT scan is currently performed with multi-slice technique that allows volumetric acquisition of the superior abdomen with multi-planar reconstruction using different methods (MPR, MIP, SSD, VR); despite this methodological innovations, CT imaging is performed with radiation exposure. On the other hand, MR is free of radiation exposure as well as provides specific information for tissue characterization using T1- and T2-weighted images as well as diffusion weighted imaging (DWI); furthermore, MRI is helpful in surgical planning for its direct multi-planarity and high contrast resolution accurately showing loco-regional lesion spread. In particular, for cystic renal masses the Bosniak classification is usually considered for imaging evaluation (12).

In our study, we evaluated in a systematic direct comparison the diagnostic accuracy of multi-slice computed tomography (MSCT) and MR regarding the identification of renal masses and the lesion characterization as benign or malignant. Our study is based on some parameters such as lesion structure, lesion margin features (regular or irregular), presence of significant or non-significant contrast enhancement, presence or absence of peri-renal fat tissue infiltration and of loco-regional vascular structures invasion. The main finding that emerged from our comparative evaluation was an absolute correlation of the results obtained with the two imaging methods; in particular, the diagnostic accuracy of both CT and MR in the identification of renal masses proved to be equal to 100% with a very good correlation between the two methods (k=1); similarly, regarding the characterization of renal masses, the diagnostic accuracy of both CT and MR proved to be equal to 90% with a high correlation between the two techniques (k=1). Only the three oncocytomas were not correctly characterized by both methods since central scar was not observed in these lesions and significant contrast enhancement was found suggesting a complete solid structure of the masses. In this regard, the diagnostic pitfalls in the differential diagnosis between oncocytoma and cancer has been widely discussed in the literature (8,14); in one of these studies (8), the authors demonstrated the ability to differentiate oncocytoma from RCC with CT of the lodges kidney through an assessment of the enhancement of the lesions in the four phases of acquisition; however, in spite of the interesting results of this study, these preliminary observations have not yet been clinically validated. Although our interesting preliminary results, some study limitations need to be mentioned and taken into consideration; first, the patient population was limited; second, in MR protocol DWI was not included; thus, additional studies in larger group using the state of art MR protocol with DWI are required to confirm our preliminary data.

However, the values of diagnostic accuracy reported in our study were similar with those reported in previous studies (9-11); in particular, some authors have suggested that in the evaluation of cystic renal masses MR shows better diagnostic accuracy than CT in identifying the number and the thickness of septa (4,10,12); this result seem to be reasonable considering the high contrast resolution of MR over CT; however this better diagnostic accuracy of MR for cystic renal masses was not observed in our group. Although in the available literature many studies have analyzed the diagnostic accuracy values of imaging techniques for the evaluation of renal masses, there are only few studies of direct and systematic comparison between different imaging techniques; the frequent finding of incidental renal masses could justify the difficulty of recruiting patients to be studied in a systematic and comparative format with different techniques. Recently, Jorns *et al.* have shown a correlation between the dimensional values of the RCC evaluated in CT and MR demonstrating how this correlation increases with the volume of the lesion (15).

Conclusions

In conclusion, the results of our study suggest that both

MSCT and MR allow accurate diagnostic evaluation of renal masses for both lesion identification and characterization as benign or malignant. MSCT is a method widely used since it easily available; however, the absence of ionizing radiation and high contrast resolution of MR represent significant advantages of this technique and it may be worth proposing its routine clinical use in all health facilities that have this equipment available.

Acknowledgements

None.

Footnote

Conflicts of Interest: Paper presented as a poster at the National Congress SIRM 2014 (PS 21-894) and EPOS (doi: 10.1594/ecr2013/C-0866) during the European Congress of Radiology (ECR), Vienna, 7-11 March 2013.

References

1. Silverman SG, Israel GM, Herts BR, Richie JP. Management of the incidental renal mass. Radiology 2008;249:16-31.
2. Hartman DS, Davis CJ Jr, Johns T, Goldman SM. Cystic renal cell carcinoma. Urology 1986;28:145-53.
3. Hartman DS, Choyke PL, Hartman MS. From the RSNA refresher courses: a practical approach to the cystic renal mass. Radiographics 2004;24:S101-15.
4. Dyer R, DiSantis DJ, McClennan BL. Simplified imaging approach for evaluation of the solid renal mass in adults. Radiology 2008;247:331-43.
5. European Network of Cancer Registries. Eurocim, Version 4.0 (European Incidence Database V2.3, 730 Entity Dictionary). Lyon, 2001.
6. Browne RF, Meehan CP, Colville J, Power R, Torreggiani WC. Transitional cell carcinoma of the upper urinary tract: spectrum of imaging findings. Radiographics 2005;25:1609-27.
7. Blitman NM, Berkenblit RG, Rozenblit AM, Levin TL. Renal medullary carcinoma: CT and MRI features. AJR Am J Roentgenol 2005;185:268-72.
8. Young JR, Margolis D, Sauk S, Pantuck AJ, Sayre J, Raman SS. Clear cell renal cell carcinoma: discrimination from other renal cell carcinoma subtypes and oncocytoma at multiphasic multidetector CT. Radiology 2013;267:444-53.
9. Pedrosa I, Sun MR, Spencer M, Genega EM, Olumi AF, Dewolf WC, Rofsky NM. MR imaging of renal masses: correlation with findings at surgery and pathologic analysis. Radiographics 2008;28:985-1003.
10. Tello R, Davison BD, O'Malley M, Fenlon H, Thomson KR, Witte DJ, Harewood L. MR imaging of renal masses interpreted on CT to be suspicious. AJR Am J Roentgenol 2000;174:1017-22.
11. Ergen FB, Hussain HK, Caoili EM, Korobkin M, Carlos RC, Weadock WJ, Johnson TD, Shah R, Hayasaka S, Francis IR. MRI for preoperative staging of renal cell carcinoma using the 1997 TNM classification: comparison with surgical and pathologic staging. AJR Am J Roentgenol 2004;182:217-25.
12. Israel GM, Hindman N, Bosniak MA. Evaluation of cystic renal masses: comparison of CT and MR imaging by using the Bosniak classification system. Radiology 2004;231:365-71.
13. Pallwein-Prettner L, Flosn D, Rotter CR, Pogner K, Syr G, Fellner C, Frauscher F, Aigner F, Krause FS, Fellner F. Assessment and characterisation of common renal masses with CT and MRI. Insights Imaging 2011;2:543-556.
14. Kang SK, Huang WC, Pandharipande PV, Chandarana H. Solid renal masses: what the numbers tell us. AJR Am J Roentgenol 2014;202:1196-206.
15. Jorns J, Thiel DD, Arnold ML, Diehl N, Cernigliaro JC, Wu KJ, Parker AS. Correlation of radiographic renal cell carcinoma tumor volume utilizing computed tomography and magnetic resonance imaging compared with pathological tumor volume. Scand J Urol 2014;48:453-9.

Cite this article as: Baldari D, Capece S, Mainenti PP, Tucci AG, Klain M, Cozzolino I, Salvatore M, Maurea S. Comparison between computed tomography multislice and high-field magnetic resonance in the diagnostic evaluation of patients with renal masses. Quant Imaging Med Surg 2015;5(5):691-699. doi:10.3978/j.issn.2223-4292.2015.07.03

